Materials and Structures/Matériaux et Constructions, Vol. **30**, June 1997, pp 269-276

SCIENTIFIC REPORTS

Tensile and flexural creep rupture tests on partially-damaged concrete specimens

A. Carpinteri[1], *S. Valente*[1], *F. P. Zhou*[1], *G. Ferrara*[2], *G. Melchiorri*[2]

(1) Politecnico di Torino, Department of Structural Engineering, 10129 Torino, Italy

(2) ENEL-CRIS, 20162 Milan, Italy

ABSTRACT

Three series of novel tensile and flexural creep tests on partially-damaged concrete specimens were carried out in order to gain some insight into creep crack growth and failure of strain-softening materials. In the tests, each specimen was initially loaded to a given point in the descending branch and thus had a lower load-carrying capacity than that at the peak-point. Then, the specimen was unloaded and reloaded to sustain a load which was from 70% to 95% of its current load-carrying capacity. Experimental creep curves display a three-stage process, consisting of primary, secondary and tertiary stages, with a decreasing, constant and increasing creep rate, respectively. The secondary stage dominates the whole failure lifetime, whereas both the secondary and tertiary stages are important in terms of creep deformation. Failure lifetime seems to be more sensitive to the change of load level in flexural tests rather than in tensile tests. The decrease in load-carrying capacity due to damage tends to result in a shorter failure lifetime and a lower critical load level for creep rupture. The descending branch of the static load-deflection or load-CMOD curve may be used as an envelope criterion for creep fracture.

RÉSUMÉ

Trois séries d'essais innovants de fluage à la traction et à la flexion ont été effectuées sur des éprouvettes de béton partiellement endommagées pour étudier la propagation de la fissuration et la rupture des matériaux radoucis. Chaque éprouvette a d'abord été chargée jusqu'à un point donné de la branche descendante, de manière à ce que sa capacité de charge soit inférieure à la charge maximale. Ensuite, l'éprouvette a été déchargée et rechargée pour supporter une charge entre 70% et 95% de sa capacité de charge existante. Les courbes expérimentales du fluage révèlent un processus en trois phases : primaire, secondaire et tertiaire, ayant une vitesse de fluage respectivement décroissante, constante et croissante. La phase secondaire domine pour la durée de vie jusqu'à la rupture, tandis que les phases secondaire et tertiaire sont importantes pour la déformation de fluage. La durée de vie jusqu'à la rupture semble être plus sensible au changement du niveau de charge dans les essais de flexion que dans les essais de traction. La réduction de la capacité de charge due à l'endommagement semble entraîner une plus courte durée de vie jusqu'à la rupture et un niveau inférieur de charge critique pour la rupture de fluage. La branche descendante des courbes statiques charge-fléchissement ou charge-CMOD peut être utilisée comme critère enveloppe pour la rupture de fluage.

1. INTRODUCTION

Strength and deformation of concrete are time-dependent and thus creep has been a subject of intensive research work. Under high sustained loading, creep rupture can occur after a certain time. However, whilst this phenomenon has been studied extensively in metals and plastic materials (Kanninen *et al.* [1]), time-dependent crack growth and failure of concrete have been investigated only to a very limited extent.

Tests of the time effects on strength and fracture may be divided into three types: loading rate, sustained loading and crack growth rate tests. Most tests on concrete fall into the first two types, although some research has been carried out on the last type (Shah *et al.* [2], Mindess *et al.* [3], Mindess [4], Tait [5]).

The results are normally presented as load level versus failure lifetime curves, strength versus loading rate curves and crack growth rate versus stress intensity factor curves. It is found that the three curves are related

Editorial note

Prof. A. Carpinteri is a RILEM Senior Member. He was awarded the Robert l'Hermite Medal in 1982 for his outstanding research work. Prof. Carpinteri is involved in the work of RILEM Technical Committees 147-FMB on Fracture Mechanics applications to anchorage and Bond and 148-SSC on Test methods for the Strain Softening response in Concrete, and participates in the Editorial Group of 090-FMA on Fracture Mechanics of Concrete - Applications. Professors A. Carpinteri, S. Valente and F. P. Zhou work at the Politecnico di Torino, Italy, a RILEM Titular Member. Dr. G. Ferrara is a RILEM Senior Member. He also participates in the work of TC 148-SSC.

0025-5432/97

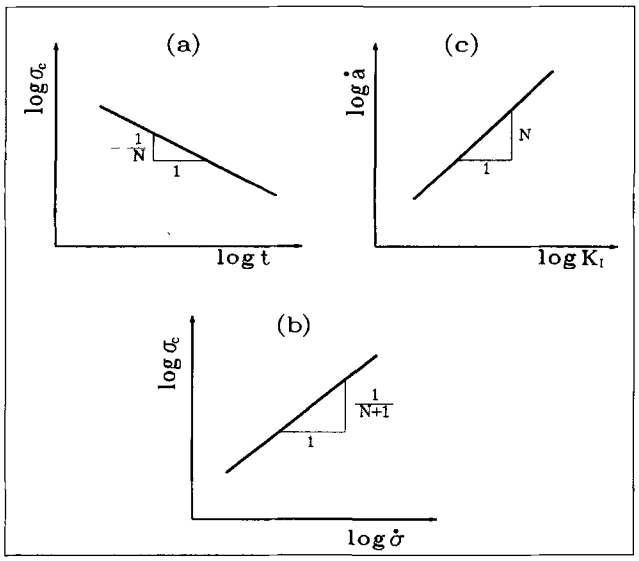

Fig. 1 – Three types of tests of time effects on the strength and fracture of concrete.

through the creep exponent N which can be evaluated from slopes, as shown in Fig. 1 (Mindess [4]). N may vary from 20 to 40 and depends on both the material and test type.

The time effects on strength and creep rupture for concrete are mainly predicted by empirical or semi-empirical equations derived from tests (Wittmann [6]). Furthermore, linear elastic fracture mechanics (LEFM) might be of little use for the creep fracture of concrete, since the damage zone in concrete is too large to apply LEFM to specimens of normal size.

During the last two decades, fracture mechanics models, such as the Fictitious Crack Model (Hillerborg *et al.* [7]), have been developed and successfully applied to the prediction of size effects on the flexural and shear strength of plain and lightly-reinforced concrete structures (Elfgren [8], Carpinteri [9], Carpinteri *et al.* [10]). Moreover, these models can predict both local behavior and global response satisfactorily. Recently, a Time-Dependent Fictitious Crack Model was developed for the creep fracture of concrete and applied to the analysis of crack growth and failure of concrete specimens in bending and compact tension by Zhou [11, 12].

Since the softening behavior (*i.e.* stress-carrying capacity decreasing with increasing deformation in the damage zone) is used as a basic law in the modeling of concrete fracture, the experimental study of creep tests on partially-damaged concrete may provide important information for the understanding and simulation of the creep fracture of concrete. Therefore, three series of tensile and flexural creep tests on concrete specimens were performed at ENEL-CRIS, Milan (see Carpinteri *et al.* [13]). The results are presented below.

Table 1 – Type of test and dimensions of specimens

Type of test	No. of tests	Specimen	Dimensions (mm)	Notch (mm)
Tensile creep	20	Notched cylinders	ϕ 100*200	10
Flexural creep Series I	18	Notched beams	840*100*100	20
Series II	22			

2. EXPERIMENTS

2.1 Test program

The experimental program includes tensile creep, flexural creep and fracture energy tests. Fracture energy tests were conducted in accordance with a RILEM recommendation [14], but with a notch depth ratio of 0.2. The geometry and dimensions of the specimens are given in Table 1.

The mix proportion of the concrete is cement : water : sand : gravel = 480:230:825:825 kg/m^3. Portland cement type 425, alluvial sand (maximum size 3.15 mm) and gravel (maximum size 10 mm) were used.

The compressive strength at 28 days is 42 MPa. The tensile strength and the fracture energy are 2.5 MPa and 132 Nm/m^2, respectively.

The age at which the specimens were tested is about 6 months. The specimens were stored at 20°C and 95% relative humidity and were tested at 20°C and 50% relative humidity.

The testing machines were Galdabini PMA of an electro-hydraulic and closed-loop type with a loading capacity of 20 and 60 tons. Deformations were measured using LVDTs of HBM W2, which have a measuring range of ± 2 mm and an accuracy of 0.2%.

The testing set-ups for tensile and flexural creep tests are shown in Figs. 2 and 3, respectively. In tensile tests, the COD (Crack Opening Displacement) was measured using three transducers. In flexural creep tests, the deflection was measured at the load application point as the mean value of two transducers, and the CMOD was measured at a point 15 mm away from the crack mouth by means of transducers.

2.2 Procedure of creep tests

The following steps (Fig. 4) were carried out in the creep tests:

Step 1. Load up to the maximum load P_{max} with deformation control (0.2 μm/s).

Step 2. Follow the softening branch until the load decreases to the prescribed value, P_D, *i.e.* unloading start load (P_D = 7.84 kN (about 60% of P_{max}) in tensile tests; P_D = 1.18 kN (about 50% of P_{max}) in flexural test series I and P_D = 1.76 kN (about 80% of P_{max}) in flexural test series II).

Step 3. Unload to about 10% of the maximum load, P_{max}.

Step 4. Reload up to a load corresponding to a certain percentage of P_D for each one of the six levels (*i.e.* 70%, 75%, 80%, 85%, 90% or 95% of P_D).

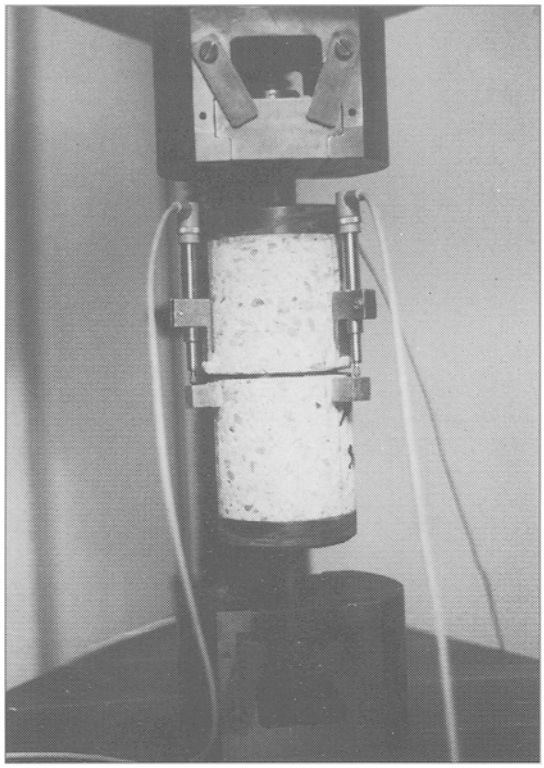

Fig. 2 – Testing set-up for tensile tests.

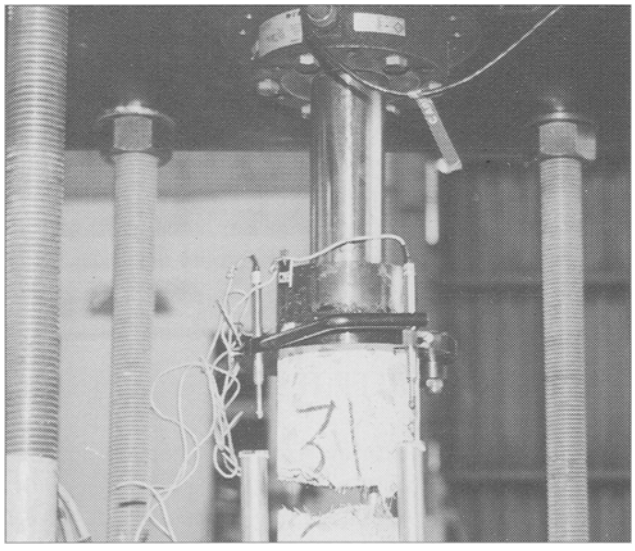

Fig. 3 – Testing set-up for flexural tests.

Step 5. The load is kept constant (± 5 N) until either creep rupture occurs or the steady creep stage is reached (*i.e.* creep rate approximately equal to zero).

Step 6. After creep rupture, the softening branch is followed, if possible.

3. TENSILE TESTS

The results of the tensile creep tests are summarized in Table 2. This table includes data on tensile strength, f_t, stress at the unloading start point, σ_D, sustained stress, σ_S, sustained load level, σ_S/σ_D, failure lifetime, t_{cr}, and ultimate creep COD, w^c_{ult}. Stress and strength values were determined by dividing the loads by the net cross-sectional area.

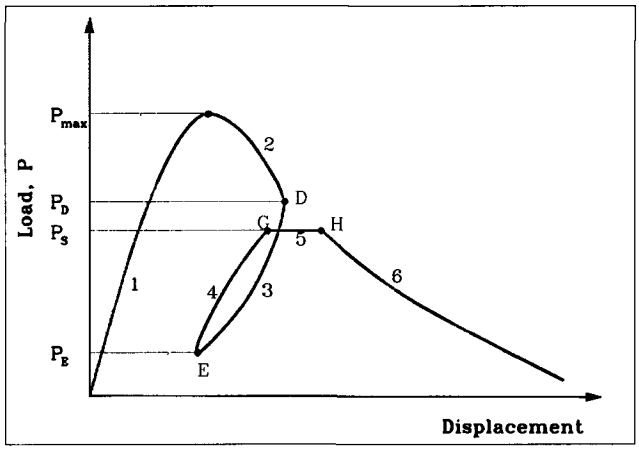

Fig. 4 – Schematic illustration of the testing procedure.

Some of the test data were left out because of incomplete details or unsuccessful tests. Even for the data included in the table, some features cannot be evaluated because of the incompleteness of the recorded data.

3.1 Tensile creep curves

Fig. 5 shows creep COD versus time curves at four sustained load levels, *i.e.* 95%, 90%, 80% and 70%, in tensile creep tests. Creep COD is defined as the difference between the current COD value and the initial COD value at the beginning of sustained loading. Normalized time (time/lifetime) is used in order to make the comparisons of creep curves more distinct.

As was the case with the creep rupture of metals in sustained loading tests, the creep curves from the present tests also display a three-stage process, according to the change of creep rate. Creep rate decreases gradually in the primary stage, is almost constant in the secondary stage

Table 2 – Tensile creep tests

Test No.	f_t (MPa)	σ_D (MPa)	σ_S (MPa)	σ_S/σ_D (%)	t_{cr} (sec)	w^c_{ult} (microns)
A1778	2.00	1.56	1.48	95	284	3.70
C1776	2.91	1.56	1.48	95	161	2.64
D1776	2.87	1.56	1.48	95	213	3.22
B1778	1.87	1.56	1.40	90	3514	3.94
D1778		1.54	1.40	90	4242	4.02
D1784680	2.48	1.56	1.32	85	12960	4.86
B1776		1.95	1.56	80	9441	5.00
C1784640	2.50	1.56	1.25	80	75601	4.70
A1784600	3.29	1.56	1.17	75	457250	10.90
B1784600	1.97	1.56	1.17	75	1307700	8.76
A1781560		1.56	1.09	70	1314400	16.10
C1782560		1.56	1.09	70	1891989*	
D1782560		1.56	1.09	70	100800	6.76

* *no failure.*

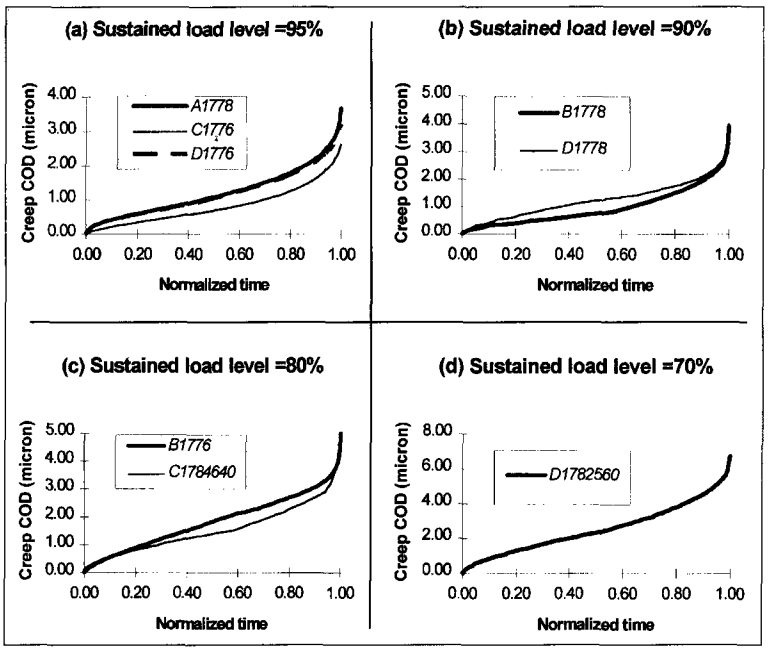

Fig. 5 – Creep curves in tensile creep tests.

and increases rapidly until failure in the tertiary stage.

In terms of failure lifetime, the primary, secondary and tertiary stages take up about 5%, 75% and 20%, respectively. In other words, the secondary stage dominates the failure lifetime in creep rupture. This feature is consistent with other similar tests, *e.g.* Reinhardt *et al.* [15].

On the other hand, creep COD growth in the primary, secondary and tertiary stages in terms of ultimate creep COD is about 10%, 40% and 50%, respectively. Put otherwise, creep COD increase in the tertiary stage is about the same as in the secondary stage. Therefore, the tertiary stage needs to be taken into due account in order to calculate the deformation accurately, even though this stage contributes much less to the whole failure lifetime.

Table 3 – Flexural creep test series I (unloading start load = 1.18 kN)

Test No.	P_{max} (kN)	P_D (kN)	P_S (kN)	P_S/P_D (%)	t_{cr} (sec)	u^c_{ult} (microns)	δ^c_{ult} (microns)
A1734	2.31	1.18	1.11	95	48	24	13
D1733	2.10	1.18	1.11	95	57	42	22
D1734	2.38	1.18	1.09	95	102	48	22
A1731	2.36	1.18	1.08	90	40	47	30
A1735	2.27	1.18	1.05	90	400	60	33
C1731	2.46	1.18	1.06	90	441	52	26
C1732	2.14	1.18	0.99	85	4382	108	58
D1731	2.27	1.18	0.99	85	2922	70	39
A1733	1.95	1.18	0.93	80	15930	152	74
B1733	2.55	1.18	0.94	80	18240	178	99
D1732	2.18	1.18	0.93	80	26904	177	98
IC1733	2.46	1.18	0.93	80	24000	106	57
B1735	2.71	1.18	0.88	75	85860	185	84
D1735	2.09	1.18	0.88	75	657000	323	169
C1734	2.29	1.18	0.82	70	1322100	304	149
C1735	2.25	1.18	0.82	70	1331100	323	143

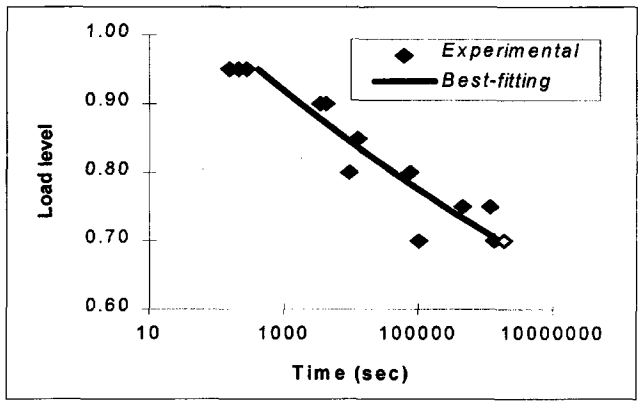

Fig. 6 – Sustained load level versus failure lifetime in tensile creep tests. Hollow diamond dot denotes the test without final creep rupture.

3.2 Sustained load level versus failure lifetime curve

Sustained load level is plotted versus failure time in Fig. 6. The best fitting equation is found to be:

$$t_{cr} = 104\left(\frac{\sigma_S}{\sigma_D}\right)^{-27} \quad (1)$$

The creep exponent from the equation above is 27 and thus comparable with the findings of other researchers. In the tests performed by Reinhardt *et al.* [15], the exponent is approximately equal to 24, whereas according to Al-Kubaisy *et al.* [16], it is 34.

The critical load level (*i.e.* the lowest level at which creep failure can occur) in the present tests cannot be determined with certainty and is estimated to be 65% to 70%. It is found to be 65% by Reinhardt *et al.* [15], about 70% by Al-Kubaisy *et al.* [16] and 75% by Domone [17].

4. FLEXURAL CREEP TESTS

Tables 3 and 4 summarize the experimental data from flexural creep test series I (unloading start load = 1.18 kN) and series II (unloading start load = 1.76 kN). The data consist of the maximum load, P_{max}, unloading start load, P_D, sustained load level, P_S/P_D, failure time, t_{cr}, ultimate creep deflection, u^c_{ult} (the superscript c means increment due to creep at a constant load), and ultimate creep CMOD, δ^c_{ult}.

Since the specimens used for the two series of tests were made from two different batches of concrete, it is necessary to check whether the properties of the materials for the two series are significantly different. Since the two series of tests are identical up to the unloading start load, we can compare the data at the peak point. As can be seen, the mean value and the standard deviation of the maximum load, P_{max}, are 2.30 kN and 0.19 kN for series I, and 2.21 kN and 0.18 kN for series II. Therefore, the mean values of P_{max} in the two series are very similar and it can be concluded that the material properties in the two series are not significantly different.

Table 4 – Flexural creep test series II (unloading start load = 1.76 kN)

Test No.	P_{max} (kN)	P_D (kN)	P_S (kN)	P_S/P_D (%)	t_{cr} (sec)	u^c_{ult} (microns)	δ^c_{ult} (microns)
A1775	2.32	1.76	1.66	95	92.5	38	40
B1775	2.34	1.76	1.66	95	14.5	11	11
C1775	2.23	1.76	1.66	95	28.5	22	23
A1776	1.94	1.76	1.58	90	2411	77	74
B1776				90	837	53	53
D1775	2.27	1.76	1.58	90	86	21	22
A1783	2.53	1.76	1.50	85	12600	61	33
C1776	2.24	1.76	1.50	85	11988	94	84
D1776	1.91	1.76	1.50	85	22230	100	84
A1779	2.08	1.76	1.41	80	108000	181	159
B1779				80	10800	113	105
D1778	2.22	1.76	1.41	80	282600*		
A1780	2.11	1.76	1.33	75	105300	174	137
C1779	2.03	1.76	1.33	75	85500	144	105
D1779	2.22	1.76	1.33	75	76500	116	87
A1781	2.14	1.76	1.23	70	667800*		
B1783	2.52	1.76	1.23	70	4999230*		
C1781	2.13	1.76	1.23	70	1188000*		

* *no failure.*

4.1 Load-deflection and load-CMOD curves

Load-deflection and load-CMOD curves from flexural creep test series I and series II are plotted in Figs. 7 and 8, respectively. Two sustained load levels, 90% and 80%, for each series are presented. Only the curves from the tests with final creep failure are included.

As might be expected, wider scatters are present on the post-peak branch than on the pre-peak branch of both the load-deflection and the load-CMOD curves, based on different tests at the same load level.

As can be observed from these curves, in each test the descending part after creep failure seems to represent a continuation of the static curve before the start of sustained loading. In other words, the unloading, reloading and sustained loading have only a local effect. The descending part of the static load-deflection or load-CMOD curve might serve as an envelope criterion for creep failure, especially for high values of P_S/P_D. This criterion implies that the fracture energy is independent of the time duration of the sustained load, as reported by Aassved Hansen [18] for three-month-old concrete specimens.

In compressive tests, the descending branch of the static stress-strain curve seems to provide a good envelope criterion for cyclic loading tests (Karsan *et al.* [19]). Moreover, for rocks, the descending part of the static curve has also been observed to be a criterion for creep rupture (Goodman [20]). It may be justified to use a similar criterion for the creep failure of concrete, since the fracture behavior of concrete and rocks is rather similar.

4.2 Creep curves

The creep deflection-time and creep CMOD-time curves from flexural creep test series I are shown in Figs. 9 and 10, respectively. Four levels, 90%, 85%, 80% and 70%, are presented. Similar curves from series II are plotted in Figs. 11 and 12, and the same four sustained load levels, 90%, 85%, 80% and 75%, are included. Creep deflection is defined as the difference between the current deflection and the deflection when the sustained loading starts. Similarly, creep CMOD is the difference between the current CMOD and the CMOD when the sustained loading starts.

Except for some tests conducted at high load levels (*i.e.* 90% and 95%), the creep curves display three stages as distinctly as in the tensile tests (Fig. 5).

In terms of failure lifetime, the primary, secondary and tertiary stages take up about 10%, 70% and 20%, respectively. In other words, the secondary stage dominates failure lifetime in creep rupture.

On the other hand, creep deflection or CMOD growth in the primary, secondary and tertiary stages is about 15%, 40% and 45%, respectively, in terms of ultimate creep deflection or CMOD. Put otherwise, the creep deflection or creep CMOD increase in the final stage is about the same as in the secondary stage. Therefore, the tertiary stage needs to be taken into account in order to accurately simulate deflections or CMOD values, even though this stage contributes much less to the whole failure lifetime.

4.3 Sustained load level versus failure lifetime curves

Sustained load level is plotted against failure lifetime for flexural test series I and series II in Figs. 13 and 14, respectively.

As usual, failure lifetime is expressed as a power function of the load level. The best fitting equation for series I is found to be:

$$t_{cr} = 9\left(\frac{P_S}{P_D}\right)^{-34} \tag{2}$$

and for series II as:

$$t_{cr} = 18\left(\frac{P_S}{P_D}\right)^{-33} \tag{3}$$

In the two equations, the exponent is about the same and only the coefficient is different. In other words, the corresponding curves (Figs. 13 and 14) present approximately the same slope, but the failure time is shorter in series I than in series II at the same sustained load level.

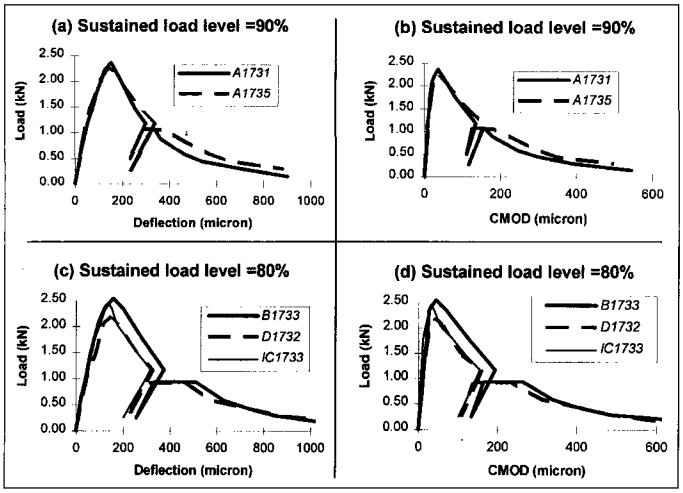

Fig. 7 – Load-deflection and load-CMOD curves in series I. Sustained load level = 90% and 80%.

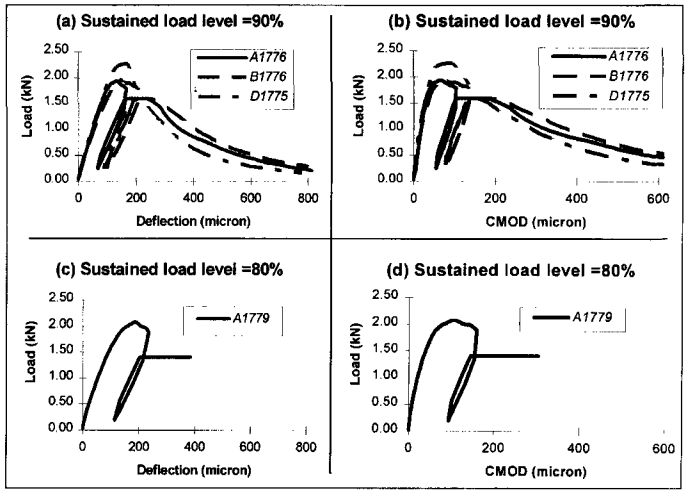

Fig. 8 – Load-deflection and load-CMOD curves in series II. Sustained load level = 90% and 80%.

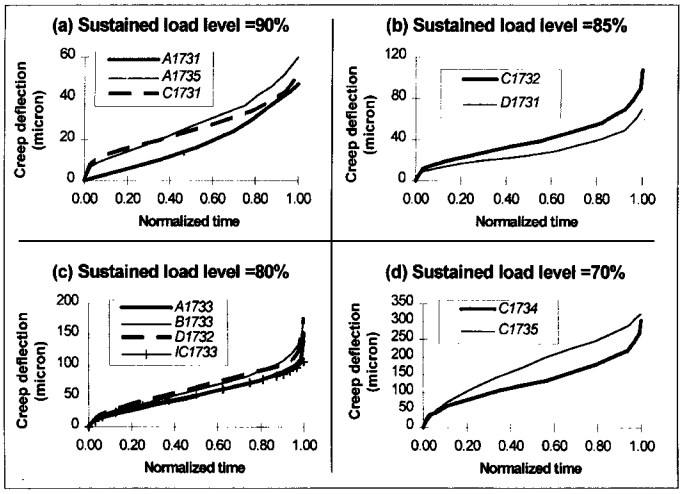

Fig. 9 – Experimental creep deflection-time curves in flexural creep series I.

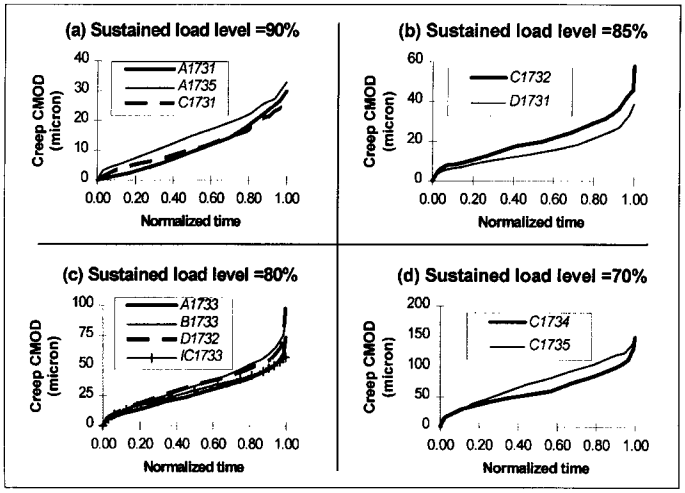

Fig. 10 – Experimental creep CMOD-time curves in flexural creep series I.

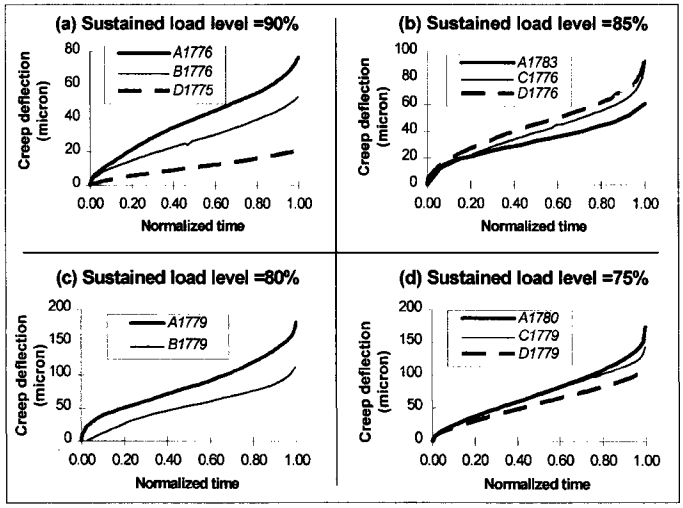

Fig. 11 – Experimental creep deflection-time curves in flexural creep series II.

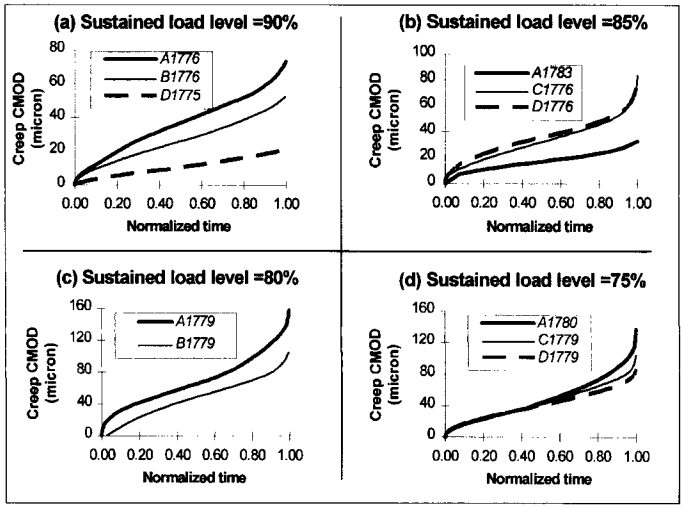

Fig. 12 – Experimental creep CMOD-time curves in flexural creep series II.

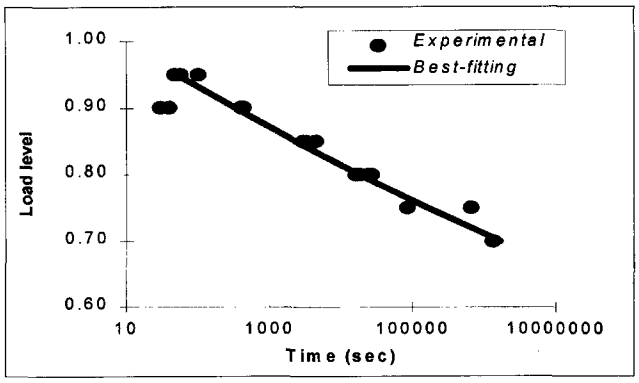

Fig. 13 – Sustained load level versus failure lifetime in flexural test series I.

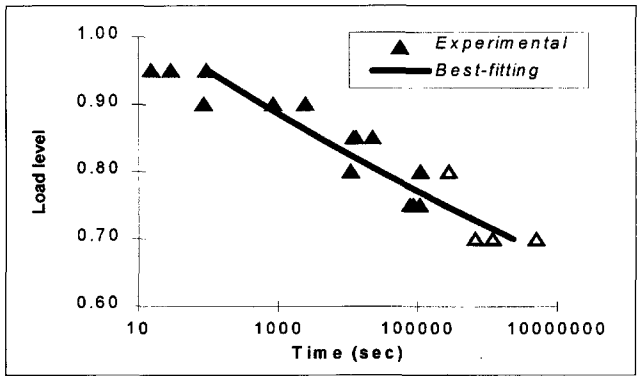

Fig. 14 – Sustained load level versus failure lifetime in flexural test series II. Hollow triangles denote the tests without final creep rupture.

The unloading start load in series I is lower than in series II. Thus, the damage zone at the beginning of sustained loading in series I is expected to be greater than in series II. The unloading start load may be regarded as the current load-carrying capacity of concrete specimens, and it is lower in series I than in series II.

Since the only difference between the two series is the unloading start load, there seems to be a trend that the increase of damage results in a shorter failure lifetime and the decrease of current load-carrying capacity gives rise to a lower capability of resisting creep fracture.

As compared with tensile tests (Fig. 6), the slope of sustained load level-failure lifetime curves in the flexural creep tests is less steep. The exponent is 27 in the tensile creep tests, and then 33 and 34 in the two flexural series. In other words, failure lifetime in the flexural tests is more sensitive to load level than in the tensile tests. This feature is consistent with the experimental evidence produced by Shkoukani [21]. He performed both a centered tensile test series and an eccentric tensile test series. It was found that the slope of sustained load level-failure lifetime curves was smaller in the latter series. It may be inferred that the slope of the curves and the parameters in the equations depend mainly on the test types.

It is difficult to determine the critical load level for series I, as creep failure occurs even at the lowest level. As for series II, it is about 70%. Therefore, the critical load level is lower in series I than in series II.

5. CONCLUSIONS

The results of tensile and flexural creep tests on partially-damaged concrete specimens are presented and analyzed.

These novel creep tests were carried out in the following way. Each specimen was loaded up to some point in the descending post-peak branch, unloaded and reloaded to a lower load than the unloading start load (which may be regarded as the current loading capacity of the damaged specimen). The load was kept constant until creep rupture or the steady creep stage (*i.e.* negligible creep) occurred.

The tests include tensile tests, flexural test series I (unloading start load = 1.18 kN) and series II (unloading start load = 1.76 kN). The main results consist of stress-deformation curves, load-deflection and load-CMOD curves, creep curves and load level versus failure time curves. These can be very useful in aiding the development of crack models and in understanding the creep fracture of concrete.

The main conclusions may be drawn as follows:

(1) Experimental creep curves display a three-stage creep process: a primary stage with a decreasing creep rate, a secondary stage with a constant creep rate and a tertiary stage with an increasing creep rate. The secondary stage dominates the whole failure lifetime, whereas both the secondary and tertiary stages are equally important in terms of creep deformations.

(2) At the same level, failure time for flexural creep test series I seems to be shorter than for series II. The critical load level (the lowest load level at which creep rupture can occur) tends to be lower for series I. It may be inferred that the capability of resisting creep rupture under sustained loading also decreases with increasing damage and decreasing load-carrying capacity.

(3) The slope of sustained load level versus failure lifetime curves seems to depend on the test types. It is approximately the same in the two flexural test series, but is steeper in the tensile tests. In other words, the failure lifetime seems to be more sensitive to the load level in flexural tests than in tensile tests.

REFERENCES

[1] Kanninen, M. F. and Popelar, C. H., 'Advanced Fracture Mechanics' (Oxford University Press, New York, USA, 1985).

[2] Shah, S. P. and Chandra, S., 'Fracture of concrete subjected to cyclic and sustained loading', *J. ACI* **67** (1970) 816-825.

[3] Mindess, S. and Nadeau, J. S., 'Effect of loading rate on the flexural strength of cement and mortar', *American Ceramic Society Bulletin* **56** (1977) 429-430.

[4] Mindess, S., 'Rate of loading effects on the fracture of cementitious materials', in 'Application of Fracture Mechanics to Cementitious Composites', edited by S. P. Shah (Martinus Nijhoff Publishers, USA, 1985) 617-636.

[5] Tait, R. B., 'Fatigue and Fracture of Cement Mortar', Ph.D.

Thesis, the University of Cape Town, Republic of South Africa, 1984.

[6] Wittmann, F. H., 'Influence of time on crack formation and failure of concrete', in 'Application of Fracture Mechanics to Cementitious Composites', edited by S. P. Shah (Martinus Nijhoff Publishers, USA, 1985) 593-615.

[7] Hillerborg, A., Modeer, M. and Petersson, P. E., 'Analysis of crack formation and crack growth in concrete by means of fracture mechanics and finite elements', *Cem. & Concr. Res.* **6** (1976) 773-781.

[8] Elfgren, L., 'Fracture Mechanics of Concrete Structures: from Theory to Practice' (Chapman and Hall, UK, 1989).

[9] Carpinteri, A., 'Application of Fracture Mechanics to Reinforced Concrete' (Elsevier Science Publishers Ltd., New York, USA, 1992).

[10] Carpinteri, A., Valente, S., Ferrara, G. and Imperato, L., 'Experimental and numerical fracture modelling of a gravity dam', in 'Fracture Mechanics of Concrete Structures', edited by Z. P. Bažant (Elsevier Applied Science, USA, 1992) 351-360.

[11] Zhou, F. P., 'Time-Dependent Crack Growth and Fracture in Concrete', Ph.D. Thesis, TVBM-1011, University of Lund, Sweden, 1992.

[12] Zhou, F. P., 'Cracking analysis and size effect in creep rupture of concrete', in 'Creep and Shrinkage of Concrete', edited by Z. P. Bažant and I. Carol (E & FN Spon, UK, 1993) 407-412.

[13] Carpinteri, A., Valente, S. and Zhou, F. P., 'Creep crack propagation in concrete structures subjected to constant loads', Research Report, Contract No. A634/93 (Dept. of Structural Engineering, Politecnico di Torino, Italy, 1994).

[14] RILEM Technical Committee 50-FMC, RILEM Draft Recommendation, 'Determination of the fracture energy of mortar and concrete by means of three point bending tests on notched beams', *Mater. Struct.* **18** (1985) 285-290.

[15] Reinhardt, H. W. and Cornelissen, H. W. A., 'Sustained tensile tests on concrete', *Baustoff* **85** (1985) Bauverlag, Wiesbaden, 162-167.

[16] Al-Kubaisy, M. A. and Young, A. G., 'Failure of concrete under sustained tension', *Cem. Concr. Res.* **27** (1975) 171-178.

[17] Domone, P. L., 'Uniaxial tensile creep and failure of concrete', *Magazine of Concrete Research* **26** (1974) 144-152.

[18] Aassved Hansen, E., 'Influence of sustained load on the fracture energy and the fracture zone of concrete', in 'Fracture Processes in Concrete, Rock and Ceramics', edited by J. G. M. van Mier, J. G. Rots and A. Bakker (E & FN Spon, UK, 1991) 829-838.

[19] Karsan, I. D. and Jirsa, J. O., 'Behaviour of concrete under compressive loadings', *J. of Structural Division* **95** (1969) 2543-2563.

[20] Goodman, R. E., 'Introduction to Rock Mechanics' (John Wiley & Sons, USA, 1980).

[21] Shkoukani, H., 'Behaviour of concrete under concentric and eccentric sustained tensile loading', *Darmstadt Concrete* **4** (1989) 223-234.